Article

Combining Chitosan Nanoparticles and Garlic Essential Oil as additive fillers to Pectin Edible Films for Primary Rice Containing

Vanessa Solfa dos Santos [1], Marcos Vinicius Lorevice [2], Graziela Solferini Baccarin [3], Fabíola Medeiros da Costa [1], Fauze A. Aouada [1] and Márcia Regina de Moura [1,*]

[1] *Hybrid Composites and Nanocomposites Group (*GCNH), São Paulo State University (UNESP), Department of Physics and Chemistry, School of Engineering, Ilha Solteira, SP, 15385-000, Brazil
[2] Brazilian Nanotechnology National Laboratory (LNNano), Brazilian Center for Research in Energy and Materials (CNPEM), 13083-970 , Campinas, SP, Brazil.
[3] Chemistry department, Center for Exact Sciences, Federal University of São Carlos (UFSCar),), Rodovia Washington Luís, Km 235, 10 SP-310, São Carlos, Brazil.
* Correspondence: Marcia Moura Dr., Phone number: +55-18-3743-1961, E-mail address: marcia.aouada@unesp.br

Abstract: Edible films were produced combining pectin (P) matrix with chitosan nanoparticle (CSNP), polysorbate 80 (T80), and garlic essential oil (GEO) as an antimicrobial agent. The CSNP were analyzed for their size and stability, and the films, throughout their contact angle, scanning electron microscopy (SEM), mechanical and thermal properties, WVP and antimicrobial activity. Four filming-forming suspension were investigated: PGEO (control); PGEO@T80; PGEO@CSNP; PGEO@T80@CSNP. The average particle size was 317nm with zeta potential reaching +21.4 mV, which indicated colloidal stability. The wettability of the films exhibited values of 65°, 43°, 78°, 64° respectively. In antimicrobial tests, the films containing GEO showed inhibition only by contact for *S.aureus*. For *E. coli*, the inhibition occurred only in films containing CSNP and by direct contact in the culture. The results indicate a promising alternative for designing stable antimicrobial nanoparticles for application in novel food active packaging.

Keywords: biopolymers; nanoparticles; garlic essential oil; packaging

1. Introduction

Biopolymers have been called as a greener and sustainable alternative raw-material to replace petroleum-based polymers in the production of food packaging (edible films and coatings), due their low toxicity, biocompatibility, renewability, and biodegradability[1]. From several biopolymers studied in the food packaging development, Pectin (PEC) have risen as an ecofriendly option for coating and film applications, due its film-forming ability, greater and greener availability from citrus fruits [2]. PEC is an anionic linear polysaccharide composed majority by α(1,4) liked D-galacturonic acid chains, being classified according to its degree of esterification: high methoxylation (HMD, when half or more of the carboxyl groups are esterified) and low methoxylation degree (LMD, when less than half of the carboxyl groups are esterified)[3]. These characteristics strongly influence physicochemical and functional properties, such as gelling conditions, solubility, temperature or even polymer modification, allowing the formation of continuous matrices for the preparation of active packaging [4,5].

Although those eco-promising properties of PEC, PEC-based films usually do not exhibit higher or comparable physical -chemical attributes than conventional packaging, which have demanded the different strategies to enhance film properties. To address these requirements, fillers and nanofillers have been successfully incorporated into PEC matrix improving mechanical, barrier and thermal properties of PEC-based composites and

 doi:10.20944/preprints202212.0435.v1

nanocomposite, respectively, in equivalent or superior order, turning these materials a useful alternative for food application[2]. Nanostructured fillers, especially polymeric nanoparticles (chitosan nanoparticles, cellulose nanofibrils, etc.) [6], have been widely inserted in the biopolymer matrices improving substantial and effectively the physicochemical properties, mechanical strength and water vapor permeability [7], as well as in some cases incorporating complementary properties, such as active properties (antioxidant and antimicrobial) [8].

Active packaging has been the focus of intense study in the last decades, and its application goes far beyond just creating a barrier between the internal and external environment. The interest relies on their capability to perform specific functions in food preservation [9]. These functions are linked to the presence of additives substances that exhibit antimicrobial activities, antioxidants, crosslinkers, or pH regulators. Recently, the incorporation of natural active compounds in food packaging has been highlighted since their consumptions have been generally recognized as safe (GRAS) by the Food and Drug Administration (FDA, USA [10]). Among these natural additives, essential oils (EO) rise as an effective alternative for having antioxidant, antimicrobial and anti-inflammatory related to the presence of terpenes, flavonoids, and other aromatic substances in their composition, besides their aroma and taste properties [11,12].

Garlic essential oil (GEO) is extracted from *Allium sativum*, an edible plant widely applied in culinary with related pharmacological and antimicrobial activities [13]. The GEO antimicrobial activity has been linked to higher quantity of sulfated substances: Allicin (Diallyl Thiosulfinate) and organosulfur compounds [12,14]. Due to the presence of these active substances, the use of GEO in the development of new active food packaging shows up as an effectively option to assist food preservation and/or to replace synthetic additives in the food industry.

Even though chitosan nanoparticles and EO have been widely describes as efficient alternative to improve, respectively, physicochemical, and active packaging properties, to date, no works combining these compounds to produce pectin-based films had been reported until. Thus, the objective of this work was to produce biodegradable biopolymer-based films containing GEO in PEC matrices, investigating the interference of chitosan nanoparticles (CSNP) and Tween 80 incorporation in terms of mechanical enhancement, hydrophobic and antimicrobial properties provided by GEO into the pectin films for application in edible packaging. The innovation of this work relies on to extend the shelf life of food, rice grains, proposing a new method of secondary active packaging containing rice.

2. Materials and Methods

Reagents used in the procedures described here were used without further purification. Chitosan (M_W= 71,3 kDa, degree of deacetylation 94%) was bought from Polymar® (Fortaleza, BR), while methacrylic acid (MAA, M_W = 86.1 kDa - CAS -79-41-4) was purchased from Aldrich (St. Louis, USA). Potassium persulphate PA ACS (270.3 g/mol) and Tween 80 (Polysorbate 80, 604.8 g/mol - CAS-9005-65-6) were bought from Dinamica Química Conteporânea Ltda® (São Paulo, BR) Garlic essential oil (*Allium sp.*; density of 1.02 $g \cdot ml^{-1}$; refraction index 1.57) was gently donated for Lapiendrius Flavours (Itaquaquecetuba, BR). The high methoxylated pectin (HMP; MD over 50%) was purchased from CP Kelco© (Limeira, BR).

2.1. Preparation and Characterization of Chitosan Nanoparticles in Solution

The CS nanoparticles (CSNP) were synthesized by polymerization of methacrylic acid (MAA) in chitosan solution according to the work firstly reported by Moura et al. 2008. This synthesis occurs in two subsequent steps: (1) CS were dispersed 0.2% (w/v) in acidic solution under (methacrylic acid 1% wt.) at constant stirring for 5 hours; (2) the solution was inserted into a reflux condenser, and potassium persulfate ($K_2S_2O_8$) as initiator was added to the CS solution. The system was kept at 70 ° C (1 hour) to promote the

Preprints (www.preprints.org) | NOT PEER-REVIEWED | Posted: 23 December 2022 doi:10.20944/preprints202212.0435.v1

polymerization of methacrylic acid. Further, the suspension was immersed in an ice bath to stop polymerization. The changes in transparency of the suspension to opalescent dispersion was the indicative of CSNP formation [15].

2.2. Chitosan Nanoparticle's Characterization: Hydrodynamic Size Distribution, Polydisperse Index and Zeta Potential

The mean size distribution, polydisperse index, and zeta potential of CSNP were obtained through dynamic light scattering in Zetasizer Nano ZS (Malvern Instruments Inc., Irvine, U.S.A). Measurements were performed in triplicate by diluting CSNP suspension (1:10) in water to avoid high light scattering rate.

2.3. Film Formulations, Preparation, and Characterization

The film-forming composition (FFC) were based on the presence of GEO, CSNP, and Tween 80 (T80). The components of the fourth different composition are fully described in Table 1 within their correlated symbols. For all the film-forming suspension (FFS), the total weight was kept constant and equal to 100g. For those composition without CSNP (PGEO and PGEO@T80), powered PEC was gently added in water at continuous mechanical stirring (~1500 rpm). GEO and/or T80 was further added, and suspension was kept at stirring for 12h. Film-forming suspension comprising CSNP, firstly PEC power was added to CSNP dispersion, followed by GEO and/or T80 incorporation. Films were prepared through casting-technique: around 40g of FFS was spread over polyester substrate (20 x 30 cm, Mylar® polyester, Dupont, USA), in which wet-thickness was controlled through doctor blade-B and left to dry for 48h at 25°C.

Table 1. Film-forming composition.

Acronyms	Pectin (% wt.)	GEO[1] (% v/w)	CSNP (% wt. pectin)	T80[1] (% wt.)
PGEO	2.0	1.0	-	-
PGEO@T80	2.0	1.0	-	1.0
PGEO@CSNP	2.0	1.0	10	-
PGEO@T80@CSNP	2.0	1.0	10	01/01/00

[1]The oil/surfactant weight ratio was equal to 1.

2.4. Water Wettability

The film water wettability was investigated through a contact angle (WCA) of water droplet (5.0 µL) over film surface via KSV Instruments (Helsinki, Finland). 60 images were recorded within 60 seconds. Measurements were taken at 5 randomly points of film surface, according to ASTM D5725-99. The WCA mean values were calculated at the right and left ends of the drop.

2.5. Scanning Electron Microscopy (SEM)

The cross-section morphology of cryogenic fracture of the films were obtained *via* Zeiss Scanning Electron Microscope (EVO LS15), operating at a voltage of 5.00 39 kV to 10.00 kV using a thin layer of gold deposited on the samples.

2.6. Fourier Transformed Infrared Spectroscopy (FT-IR)

The FT-IR spectra were recorded in spectrophotometer (Nicolet – NEXUS 670 FT-IT), operating in 128 scans, frequency range of 400 – 4000 cm^{-1}, and 2 cm^{-1} of resolution. Films were macerated and pressed into KBr pastilles.

2.7. Mechanical Properties: Tensile strength, Strain, and Young's Modulus

 doi:10.20944/preprints202212.0435.v1

Firstly, the film thickness was determined at five random positions along the sample using digital micrometer No. 7326 (Mitutoyo Corp., Japan). The thickness means were further used in mechanical and barrier analysis.

The mechanical attributes of Tensile Strength (TS), Strain (%), and Yong's modulus (E) were calculated from a uniaxial test according to ASTM method D882-12 [16] through an Instron Universal Testing Model 3369 (Instron Corp., USA). At least ten samples of each film in the dimensions of 100 mm length × 13 mm width were cut and analyzed. The films were equilibrated at 33 ± 2% relative humidity (RH) for 48 h before test.

2.8. Water Vapor Permeability

The water vapor permeability (WVP) was evaluated according to the ASTM E96-80 [17]with some modifications. Briefly, the film samples were cut into a circular format and placed on poly(methyl methacrylate) cups, which were filled with deionized water, so the films acted as a semipermeable barrier between a high- and a low-RH environment. To determine the RH at films' undersides (%) and water permeability (g mm KPa^{-1} h^{-1} m^{-2}), the test cells had their weights measured every two hours for 24h at 25º ± 1 C.

2.9. Thermal Property: Thermogravimetric Analysis

The thermal degradation analysis was performed in a Thermogravimetric Analyzer TGA-Q500 (TA Instruments, New Castle, DE, USA). The measurements were recorded in the temperature range of 20 to 800 ◦C (heating rate of 10 ◦C/min). The nitrogen flow was maintained at 100 mL/min.

2.10. Antimicrobial Properties

Antimicrobial activity was evaluated based on disk inhibition tests as fully described by Otoni *et al.* [18]. Briefly. The disk inhibition test was performed as following: colonies isolated from the cultures of *E. coli* (ATCC 25922) and *S. aureus* (ATCC 25923) were inoculated into 0.85% (w/v) NaCl solution until 0.5 McFarland standard turbidity atched (10^8 CFU mL^{-1}. The suspensions were spread out over solidified Mueller Hinton agar. Discs with diameters of 0.5; 0.6; 0.7 and 0.8 cm were exposed to UV light (110 V and 254 nm) for 2 min on each side before being placed in contact with the bacterial surface and the plates were incubated at 37 ° C for 24 h in the appropriate incubation chamber. The inhibition zones (diameters around the films) were measured to the nearest 0.01 mm with a digital caliper (Mitutoyo Corp.). The inefficient in inhibiting microbial growth was considered as when inhibition zones were not detected, and the area was assigned as zero.

3. Results

This section may be divided by subheadings. It should provide a concise and precise description of the experimental results, their interpretation, as well as the experimental conclusions that can be drawn.

3.1. CNPS Characterization

The particle size distribution is an important characteristic of nanoparticles since the size is an essential factor that drives their good performance when incorporated into a polysaccharide-based matrix. The mean size obtained for CSNP was 317 ± 2 nm. Aranda-Barradas et al. [19] reported regardless the others factors that can affect the diameter of the particles (CS content or MMA precursor, for instantce), chitosan-based systems prepared through via insitu polymerizations or the precipitation of preformed polymers usually provide CSNP size diameters ranging from 50 to 300 nm. According to Moura et al. [12], the CSNP is usually spherical and stable. This stability can be measured through zeta potential. Here CSNP exhibited zeta potential of 21.4 ± 0.9 mV, indicating indicating a stable suspension and since the values are between in modulu, 20 to 40 mV. In the case of NPQs, this increase is related to the amount of chitosan, consequently, there will be an

Preprints (www.preprints.org) | NOT PEER-REVIEWED | Posted: 23 December 2022 doi:10.20944/preprints202212.0435.v1

increase in the concentration of NH3+ ions, resulting in a greater surface positive charge [20] .

3.2. PectinGEO Films Characterization

3.1.1. Visual Appearance

Figure 1 summarizes the data on visual, superficial, and internal film structure. From Figure 1a-d, differences in the film appearance can be noted when the first Tween 80 and/or CSNP was incorporated. PGEO@T80 films seemed more flexible than PGEO, indicating that the surfactant could be plasticizing the pectin matrix or even facilitating some compatibilization of GEO hydrophobic components with the polysaccharide matrix. Interestingly, CSNP turned the film extremally homogeneous and apparently more flexible than PGEO. Also, less transparency may be linked to a less crystalline portion of pectin when the nanofiller is added. This behavior was not observed when Tween 80 was added to the film composition, however, even looking more brittle than PGEO@CSNP, PGEO@T80 and PGEO@T80@CSNP look similar, without fissures or phase separation, revealing the good compatibilization of these three components (GEO, T80, and CSNP) with the polymeric matrix.

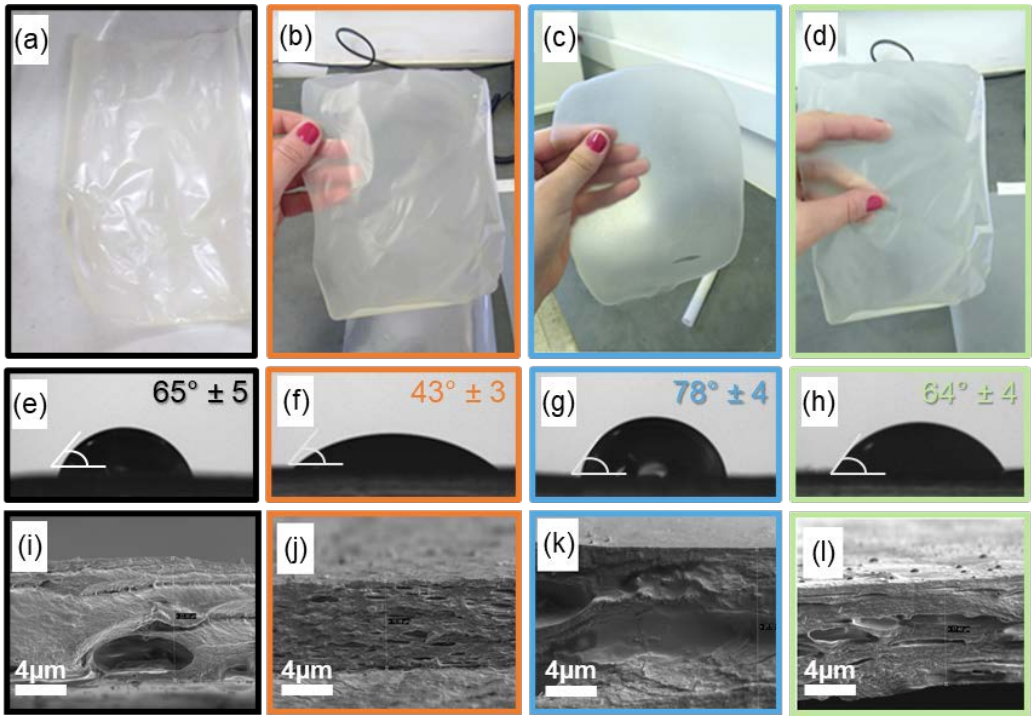

Figure 1. Visual (a-d), superficial (e-h), and internal SEM (i-l) characteristics of pectin-based: PGEO(a, e, and i); PGEO@T80 (b, f, and j); PGEO@CSNP (c, g, and k); PGEO@T80@CSNP (d, h, and l).

3.1.2. Water Wettability

The water contact angle (WCA) measurement gives the wettability (hydrophilic/hydrophobic nature) of the surface of the films. Values above 90° indicate surfaces intrinsically hydrophobic, while values below 90° suggest more hydrophilic surfaces [21]. The results can be seen in Figure 1e-h. All films have shown hydrophilic surfaces, with the PGEO film (Figure 1e) showing WCA of 65°. By adding surfactant Tween 80 (Figure 1f), the WCA decreased to 43°, indicating that maybe this compound provided greater affinity between its surface and the liquid, turning it more hydrophilic. This may be correlated to a possible plasticizing effect of the surfactant in the matrix, where the hydrophilic part of the surfactant interacts with water, facilitating its presence between the polymer chains[22]. In this way, there is a decrease in the polymer-polymer interactions, and also

 doi:10.20944/preprints202212.0435.v1

the migration of the excess to the surface, increasing the hydrophilicity of the film [22]. Equally, the film containing the CSNP (Figure 1g) exhibited WCA equal to 78°, but when Tween80 (Figure 1h) was added, the WCA reached 64°. Even CSNP may provide the film with a denser matrix caused by favoring the aggregation of hydrophobic agents present in the essential oil during the drying process [23,24]. In general, although all compositions contain GEO, the compositions incorporated with Tween 80 showed low hydrophobicity, considering that the surfactant mediates the oil/water interface, hindering the hydrophobic effect in the mediations of the film surface. Given the results, it is possible to affirm that the chemical composition of the material directly influences the hydrophobic characteristics of the final film.

3.1.3. Internal Morphology: SEM analysis

The cryogenic fracture micrograph of the films intended to investigate the effect of the nanofiller and the surfactant in the films containing GEO. Figure 1i-l shows the cross sections of the pectin-based films. The control film GEO (Figure 1i) presented a compact and ordered structure, suggesting miscibility among some components of the EO and pectin matrix. In films containing Tween 80 (Figure 1j), internal pores with variable dimensions distributed randomly within the matrix can be observed, which could reduce hydrophobic aspects and increase flexibility, providing the film with a more amorphous structure [25,26]. When CSNP were incorporated into the film composition (Figure 1k), the polymeric matrix presented a denser and more compacted than the control film (Figure 1i). The uniformity of its internal structure and the decrease in pore size indicate that CSNP acted as reinforcing agents.

3.1.4. FT-IR analysis

Figure 2 shows the infrared spectra of the different film compositions and their components. The spectrum of the GEO (Figure 2a) shows the typical four bands in the region between 3100 and 2900 cm -1. The first at 3081 cm-1 corresponds to the asymmetric stretching vibration of CH2, the second (3011-3007 cm- 1) relates the C-H stretching, the third (from 2980 to 2978 cm- 1) shows the symmetric stretching vibration of CH2, and the fourth between 2914 and 2912 cm -1 the stretching of - CH 2 -. The band 1428 and 1401 cm -1 are attributed to the stretching of -CH 2 -, and at length 1217 cm -1 concerns the stretching CH 2 = CH-, which are associated with the presence of GEO in the films [8,13,27].

Figures 2a and 2b show the infrared spectra of the neat CS and the CSNP, respectively. The band between 1657 cm-1 and 1598 cm-1 refers to the amine group of the CS structure, which is shifted (1638 and 1545 cm-1) due to the interaction among the amine group of CS (NH+3) and the carboxylic groups (COO-) from PMMA. The broad band at 3419 and 2859 cm-1 assigned to asymmetric/symmetric stretching of the primary amines (NH2) and O–H stretching from intermolecular/intramolecular hydrogen bonds) [13,27]. Moreover, peaks at 1750 cm-1 and 1640 cm-1 are assigned to the stretching of carboxylate ions COO-. In addition, the weaker symmetric COO- stretching is followed by moderately intense absorption patterns between 1300 and 800 cm-1, a pectin-fingerprint region, also visualized in the spectra of the films (Figures 2b).

Preprints (www.preprints.org) | NOT PEER-REVIEWED | Posted: 23 December 2022 doi:10.20944/preprints202212.0435.v1

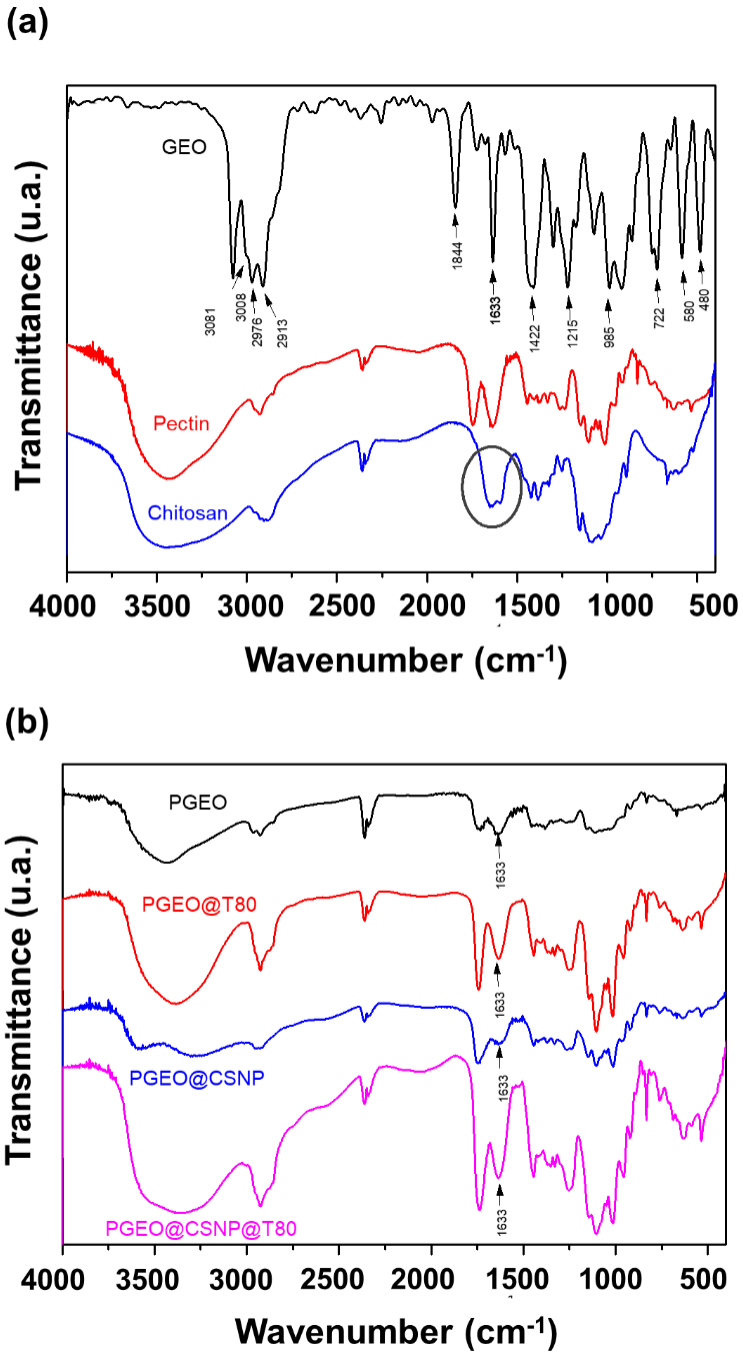

Figure 2. Infrared spectra of (**a**) films compositions: garlic essential oil (GEO, black), pectin (P, red, and chitosan (CS, blue); (**b**) pectin-based films: PGEO (black); PGEO@T80 (red); PGEO@CSNP (blue); PGEO@T80@CSNP (pink).

3.1.4. Mechanical Properties

The mechanical properties are one of the most important properties of composite films, which can be evaluated in terms of tensile strength (TS), Young's modulus (YM) and elongation at break (EB). The TS represents the film's resistance when it is submitted to tensile forces, and modulus of elasticity provides quantitative values of film stiffness [28,29]. In this context, the addition of chitosan nanoparticles and/or surfactant in the pectin matrix with garlic essential oil was investigated and how it could impact on the mechanical performance of the pectin-based films. Figure 3a-d shows the results obtained from the mechanical properties for the different film formulations. The tensile strength, elongation at break and Young's modulus ranged from 13.84 to 29.03 MPa, 2.55 to 1.6%

Preprints (www.preprints.org) | NOT PEER-REVIEWED | Posted: 23 December 2022 doi:10.20944/preprints202212.0435.v1

and 1.32 to 2.1 GPa, respectively. The values of tensile strength and Young's modulus of the control film (PGEO) had a positive significant difference ($p < 0.05$) in relation to the other compositions, with variation of up to 47.67 % and 62.9 %, respectively. The PGEO composite was the stiffness film. On the other hand, the elongation at break had no difference among the film composition.

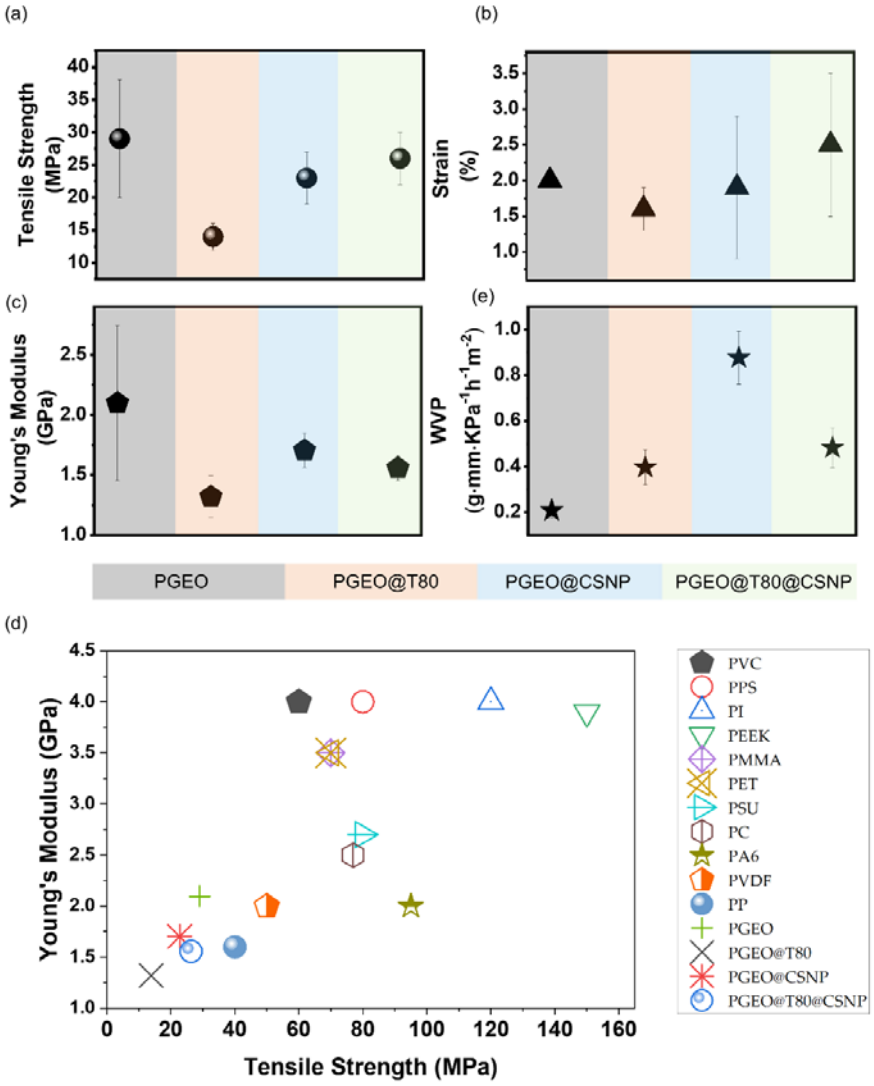

Figure 3. Mechanical properties (tensile strength, Young's modulus and elongation at break) for different film formulations.

The main drawback of pectin-based films in applications relies on their limited mechanical properties, as they become, under specific drying conditions more rigid, brittle and have low elongation at break (EB < 25 %) [30–33]. Thus, the increment in such properties is essential. to improve their applicability. It has been reported that several phenolic compounds, essential oil extracted from plants, are used to improve the functional properties of biopolymers [34–37]. In addition, they also describe antioxidant activity to these films, being an extra property to extend the shelf life of foods, reduce food waste and limit the application of synthetic chemicals, thus meeting the goals of sustainable industrial and social development [38].

Although it does not vary statistically, the material shows an improvement tendency. By adding CSNP it is possible to observe an increase in the elongation, which can be related to the composition PGEO@T80@CSNP in relation to the control film (PGEO). And the insertion of CSNP to the PGEO@T80 film increased the TS, YM and EB. Yeddes *et al.*

 doi:10.20944/preprints202212.0435.v1

[39] described the tensile strength values of films with different proportions of chitosan and pectin, however the tensile strength of composite films had a threefold increase when the proportion of chitosan was increased from 3 to 5 parts. The high tensile strength values of these films can be attributed to the excellent association between the NH3+ groups of chitose and the COO− groups of pectin [39]. Kurek *et al.* [29] concluded in their studies that chitosan flexibility may be caused by the presence of β-(1–4)-D-glucosamine bonds that are absent in pectin polymer chains.

Norcino *et al.* [40] showed that the addition of copaiba oil nanoemulsions to pectin films led to a considerable increase in EB, with pure pectin films showing elongation around 1%, with a concomitant decrease in TS. They suggested that the plasticizing action of copaiba oil could lead to a decline in intermolecular interactions between the pectin chains and increase the free volume and mobility of the chain, which would eventually form a film with lower strength and greater flexibility. They also attributed the lower TS of the films to the formation of a heterogeneous and incoherent structure in the films caused by the copaiba oil phase.

The addition of the surfactant caused a significant reduction ($p < 0.05$) in the tensile strength when added only to the control film (PGEO). This behavior was also reported by Brandelero, Yamashita and Grossmann [41], cassava starch films with Tween 80 showed a reduction in mechanical strength values due to the plasticizing effect of the surfactant, increasing the free volume between adjacent starch chains and making the more fragile structure. Tween 80 is a hydrophilic surfactant with a higher hydrophilic-lipophilic balance value and can interact with water that weakens the intermolecular hydrogen bond, consequently resulting in decreased mechanical properties [42].

Figure 3d shows a comparison of Young's modulus and tensile strength (Omnexus) with petroleum-based synthetic polymers that are commonly used as packaging. It can be observed that the biopolymers synthesized in this work have elastic modulus and tensile strength values similar to PVDF and PP. Therefore, biopolymers can be applied in packages that require mechanical resistance, such as these synthetic polymers.

3.1.5. Water Vapor Permeability

The edible films' water vapor permeability shows dependency on the biopolymeric-based matrix used, and their values are still much higher than those of petroleum-based polymeric matrices. Thus, it is imperative to improve this property to turn them comparable to conventional polymeric matrices. Figure 3e shows the WVP results for the different compositions. The PGEO film exhibited a WVP value of 0.21 g mm K^{-1} h^{-1} m^{-2} below WVP values (0.6 - 1.05 g mm K^{-1} h^{-1} m^{-2}) reported in pectin-based films [43]. This result may be related to both the nature of the matrix and the hydrophobicity of the GEO. The polymers chains interact with EO compounds, which may reduce the availability of hydrophilic groups to form hydrophilic bonds, thus decreasing the water vapor transmission rate of the film [44–47]. Due to the hydrophilic character of the matrix, the water molecules interact with the polar groups of the polymer chains and get trapped by Van der Waals interactions as illustrated in Figure 4a.

Preprints (www.preprints.org) | NOT PEER-REVIEWED | Posted: 23 December 2022 doi:10.20944/preprints202212.0435.v1

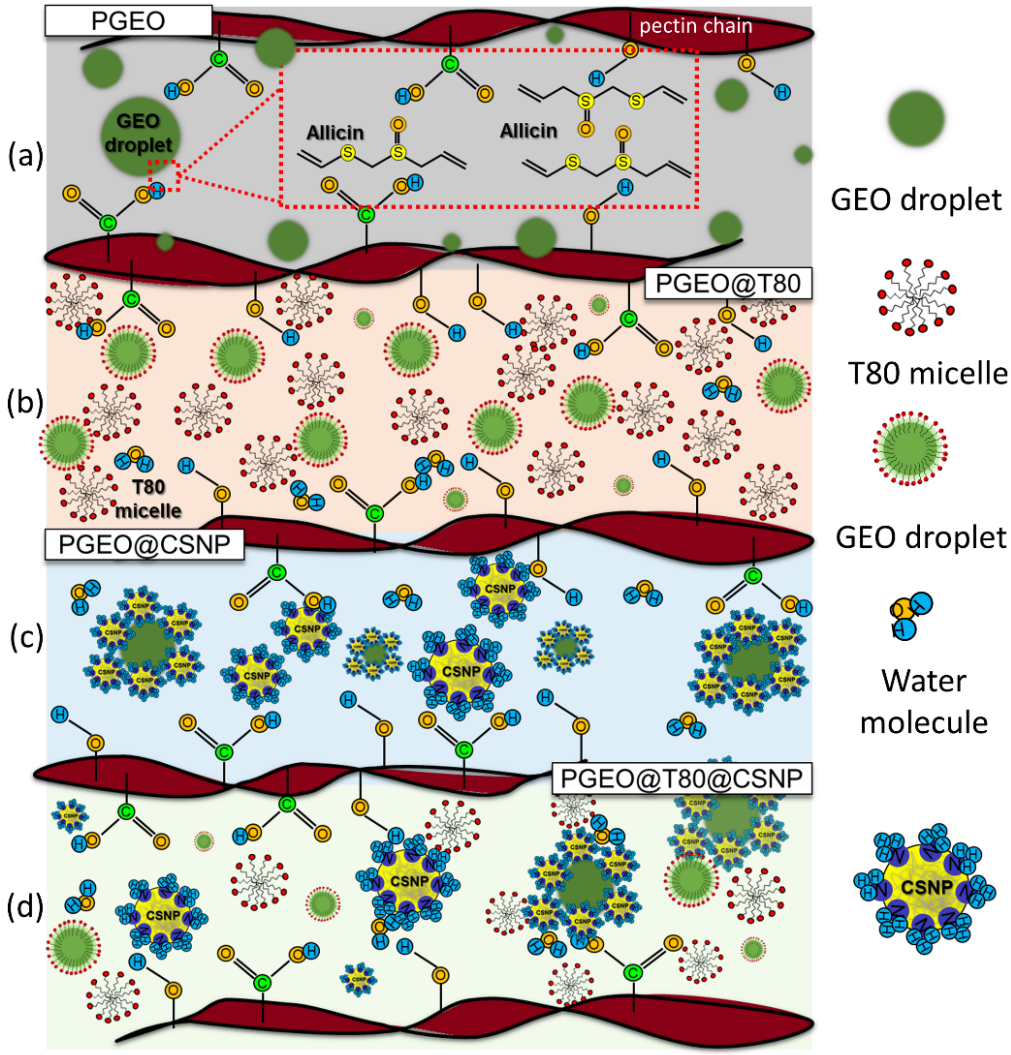

Figure 4. Proposed mechanism of garlic essential oil (GEO), surfactant Tween 80 (T80), and chitosan nanoparticles (CSNP) distribution in pectin matrix. Pectin incorporated with GEO (a), GEO@T80 (b), GEO@CSNP (c), and GEO@T80@CSNP.

In the films containing the surfactant (Figure 3e), the WVP values increased to 0.39 g mm K^{-1} h^{-1} m^{-2}. This increase can be linked to the presence of the surfactant [48]. Tween 80 molecules probably increase the narrow spacing between the pectin chains, allowing greater diffusion of water molecules (Figure 4b). The non-free groups favor greater mobility, and consequently, the permeability of the water molecules, such iterations can be observed in the representative model in Figure 4c for the films containing Tween 80 [41].

The CSNP incorporation (Figure 3e) reached WVP value up to 0.87 g mm K^{-1} h^{-1} m^{-2}. This unexpected increase may be related to the film thickness. The barrier properties of films depend on factors such as thickness and plasticizer concentration. McHugh *et al.*[17]observed that as film thickness increased. The film provided greater resistance to mass transfer through it; consequently, the equilibrium water vapor partial pressure at the internal surface of the film increased. It caused an improvement on permeability due to the higher HR gradient between the film and the environment [49,50]. Additionally, the surface positive of CSNP interacting with the polar groups of the pectin matrix turned these groups no longer free to interact with water molecules. Then, there may be a repulsive interaction between the CSNP surface and the positive permanent dipoles of the water molecules (hydrogens) promoting diffusion between all formulations, as represented in Figure 4d.

Preprints (www.preprints.org) | NOT PEER-REVIEWED | Posted: 23 December 2022 doi:10.20944/preprints202212.0435.v1

3.1.6. Thermogravimetric Analysis

Thermal analysis is an efficient technique to evaluate the thermal stability of films. The thermograms of the pectin-based films are shown in Figure 5.

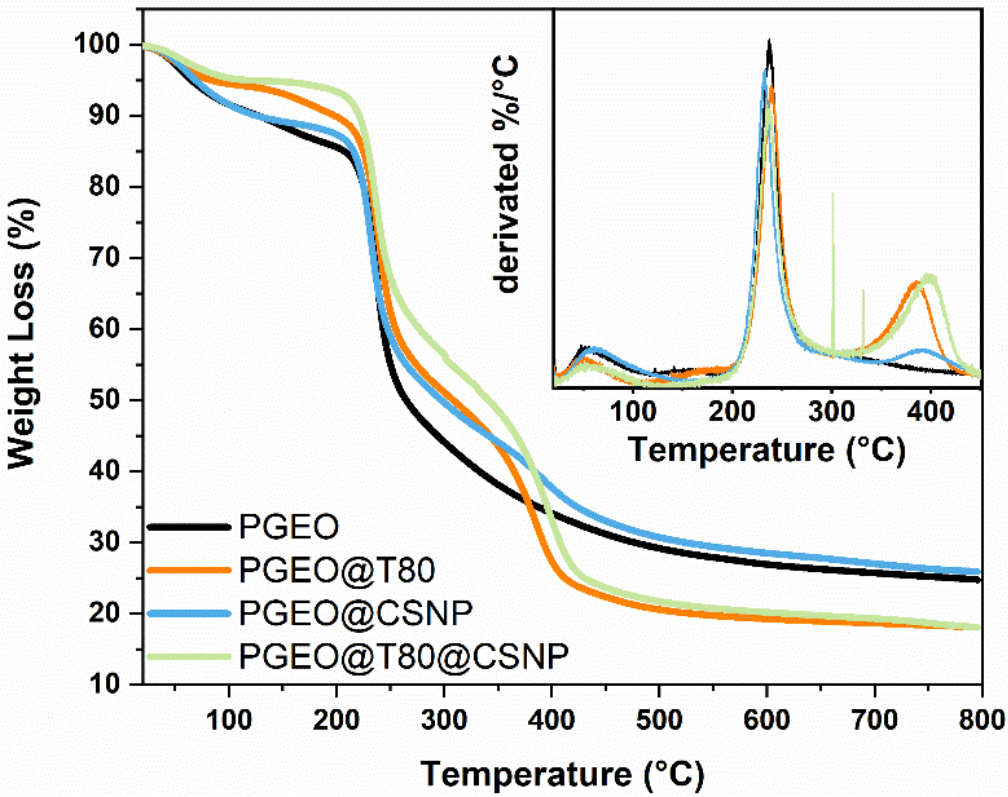

Figure 5. Thermogravimetric scans of composites (PGEO and PGEO@T80) and nanocomposite (PGEO@CSNP and PGEO@CSNP@T80) films.

Generally, the degradation profile of biopolymer-based materials occurs in three stages: dehydration of the material (up to 100 °C) that is naturally retained in the matrix, irreversible degradation of saccharides (~230°C), and thermal deterioration of organic compounds into CO2 and H2O above 230°C[41,45–51].Here, a typical initial weight loss stage over 100 °C was observed in all thermogram curves. The presence of T80 added a second weight loss step, probably related to surfactant degradation can be noted [45,52]. The degradation onset temperature (Td) decreased to 87.73°C when compared to the thermogram of the PEC matrix. This suggests that the addition of the surfactant decreased the molecular interactions between the adjacent pectin chains made up of hydrogen bonds between the hydroxyl groups of the PEC. Similar results were mentioned by Norcino *et al.* [40], who reported a decrease in the temperature of onset of degradation (Td) for films containing copaiba oil emulsified with Tween 80 when compared to pectin. Such results were also reported with the addition of extracts in the film composition as reported in the literature[53,54]. Interestingly, the addition of T80 decreased the water moisture, being even higher when CSNP was incorporated into the polysaccharide matrix, which turned the nanocomposite matrix more thermal stable. For the films containing the CSNP, a slow mass loss occurs from 140 °C to 200 °C referring to the decomposition of polymer with low molar mass as NH3+ [55]. At approximately 243 and 325 °C the onset of degradation (TD) occurs, this event corresponds to the process of dehydration of the anhydrous glucosidic ring present in the chitosan molecule, depolymerization, and side chain decomposition [54,56].

3.1.7. Antimicrobial Properties

 doi:10.20944/preprints202212.0435.v1

The antimicrobial activity of the films was analyzed through an inhibitory halo against *E. coli* and *S. aureus* since these microorganisms are the most common pathogens found in food (Figure 6) [30,57]. The inhibition against E.coli occurred by contact in the films containing the CNPs. The results suggest that chitosan content drives inhibitory activity, and since this polysaccharide is assembled as nanoparticles, the effect may have been intensified. Additionally, as the nanostructures have a large surface area, the ionic interaction of the bacterial cell wall and CSNPs was enhanced, and then the antimicrobial property. It promoted cell rupture, changing the membrane permeability, inhibiting the replication of the bacteria DNA, and causing cell death [54,56,58].

GEO content and T80 did not show an inhibition effect (Figure 6). It may be related to the GEO volatile compounds, evaporating themselves even before diffusion on the Agar, leading to a decrease in the antimicrobial property of the film. The Agar plate method has already been related to greater exposure of these compounds present in GEO (sulfides) to the environment, decreasing the antimicrobial activity of GEO and turning it undetectable [59]. In addition, Gram-negative food spoilage bacteria and foodborne pathogens such as E.coli show higher resistance to various types of EOs due to the complexity of their structure, thus explaining the unsatisfactory antimicrobial effect of the films [11,60]. On the contrary, both CNPs and GEO drove the inhibitory activity of the films for the S. aureus bacteria. Previous studies have reported a more synergic effect of chitosan and EOs against Gram-positive bacteria than Gram-negative bacteria due to the difference in the outer membrane characteristics. These finds explain why all films showed inhibitory activity against S.aureus while for E.coli only those containing CNPs were effective in inhibition [11,61]

 doi:10.20944/preprints202212.0435.v1

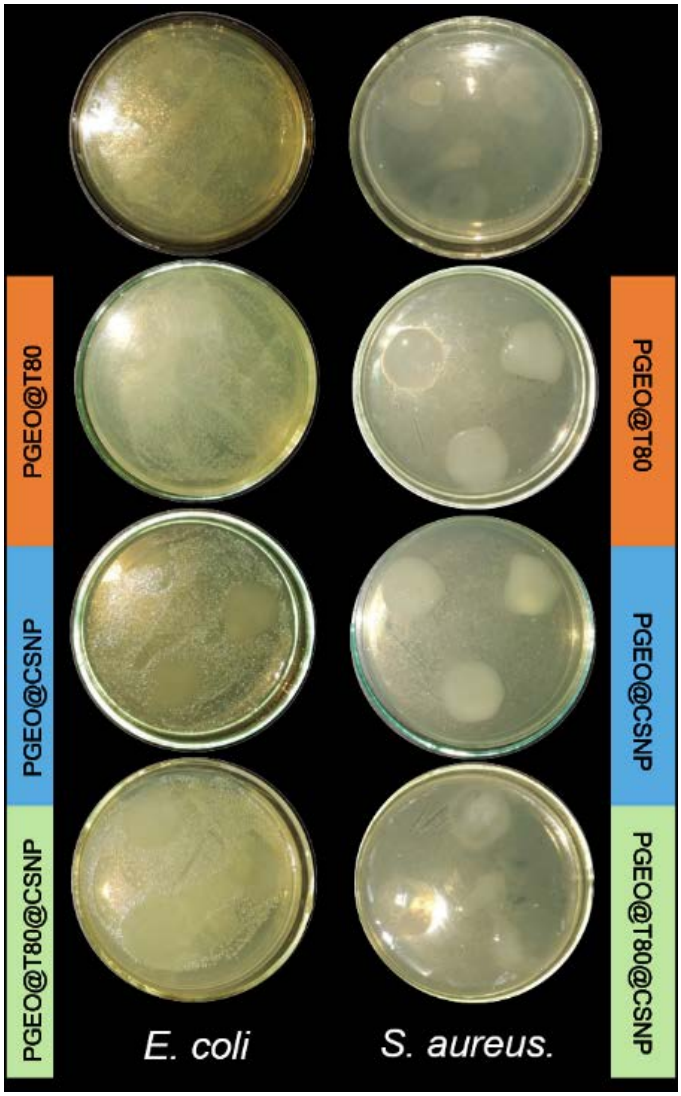

Figure 6. Antimicrobial activity of the films analyzed through an inhibitory halo against *E. coli* and *S. aureus.*

Among several novel packaging with the potential to reach the final consumers, active packaging is a promising way to slowly release functional additives to the food and avoid food spoilage. Moreover, considering the growing concerns about reducing the disposal of plastics in the environment, the suggested applications for biopolymer films based on the results obtained in this work expand the applications already reported for active and edible films.

4. Conclusions

According to the results obtained in this work, it can be concluded that the NPQs was stable as shown by the Zeta potential data. Their presence in the composition of the films caused a decrease in the surface affinity of the film for water, thus increasing its hydrophobicity, results confirmed by scanning electron microscopy images. The SEM analysis showed the uniformity of its internal structure indicates that CSNP acted as reinforcing agents. This reinforce improved is demonstrated in mechanical properties results.

The results from the antimicrobial activity showed that all films containing NPQs presented inhibition only by contact for Gram-positive bacteria (*S.aureus*) and Gram-negative (*E.coli*). For films containing essential oil and nanoaprticles, the synergistic effect of oil and nanoparticle contributed to the improvement of inhibitory activity against *S. Aureus*. For bacteria of the *E.Coli* type, only the films containing nanoparticles were more

active. In general, the films presented properties considered satisfactory for application as active edible films, demonstrating homogeneous and continuous appearance, as well as slight transparency and malleability.

Acknowledgments: Department of Physics and Chemistry of São Paulo State University (UNESP) for the financial support provided. This study was financed in part by the Coordenação de Aperfeiçoamento de Pessoal de Nível Superior - Brasil (CAPES) - Finance Code 001. 2019. F. A. Aouada thanks the Brazilian National Council for Scientific and Technological Development (CNPQ; Grant No. 312414/2018-8). M. R. de Moura thanks the São Paulo Research Foundation (FAPESP) (Grant 2019/06170-1 and 2013/07296-2 CEPID). M. R. de Moura thanks the Brazilian National Council for Scientific and Technological Development (CNPQ; Grant No. 315513/2021-7).

Author Contributions: Vanessa S. dos Santos: Conceptualization, Methodology, Validation, Investigation, Writing - original draft, Project administration. Marcos V. Lorevice: Methodology and Investigation; Writing - review & editing; Validation. Graziela Solferini Baccarin: Writing - review & editing; Validation. Fabíola M. da Costa: Methodology; Validation; Investigation. Fauze A. Aouada: Conceptualization; Methodology; Supervision; Funding acquisition. Marcia R. de Moura: Conceptualization, Methodology, Validation, Investigation, Writing – original draft, Writing - review & editing, Supervision, Resources, Project administration, Funding acquisition.

References

1. Mollah, M.Z.I.; Akter, N.; Quader, F.B.; Sultana, S.; Khan, R.A. Biodegradable Colour Polymeric Film (Starch-Chitosan) Development: Characterization for Packaging Materials. *Open Journal of Organic Polymer Materials* **2016**, *06*, 11–24, doi:10.4236/ojopm.2016.61002.
2. Mellinas, C.; Ramos, M.; Jiménez, A.; Garrigós, M.C. Recent Trends in the Use of Pectin from Agro-Waste Residues as a Natural-Based Biopolymer for Food Packaging Applications. *Materials* 2020, *13*.
3. Lam, M.; Shen, R.; Paulsen, P.; Corredig, M. Pectin Stabilization of Soy Protein Isolates at Low PH. *Food Research International* **2007**, *40*, 101–110, doi:10.1016/j.foodres.2006.08.004.
4. Kastner, H.; Einhorn-Stoll, U.; Senge, B. Structure Formation in Sugar Containing Pectin Gels – Influence of Ca2+ on the Gelation of Low-Methoxylated Pectin at Acidic PH. *Food Hydrocoll* **2012**, *27*, 42–49, doi:10.1016/J.FOODHYD.2011.09.001.
5. Galus, S.; Lenart, A. Development and Characterization of Composite Edible Films Based on Sodium Alginate and Pectin. *J Food Eng* **2013**, *115*, 459–465, doi:10.1016/J.JFOODENG.2012.03.006.
6. Spricigo, P.C.; Pilon, L.; Trento, J.P.; de Moura, M.R.; Bonfim, K.S.; Mitsuyuki, M.C.; Mattoso, L.H.C.; Ferreira, M.D. Nano-Chitosan as an Antimicrobial Agent in Preservative Solutions for Cut Flowers. *Journal of Chemical Technology and Biotechnology* **2021**, *96*, 2168–2175, doi:10.1002/jctb.6766.
7. Antoniou, J.; Liu, F.; Majeed, H.; Qi, J.; Yokoyama, W.; Zhong, F. Physicochemical and Morphological Properties of Size-Controlled Chitosan–Tripolyphosphate Nanoparticles. *Colloids Surf A Physicochem Eng Asp* **2015**, *465*, 137–146, doi:10.1016/J.COLSURFA.2014.10.040.
8. Lorevice, M.V.; Otoni, C.G.; de Moura, M.R.; Mattoso, L.H.C. Chitosan Nanoparticles on the Improvement of Thermal, Barrier, and Mechanical Properties of High- and Low-Methyl Pectin Films. *Food Hydrocoll* **2016**, *52*, 732–740, doi:10.1016/j.foodhyd.2015.08.003.
9. Vianna, T.C.; Marinho, C.O.; Marangoni Júnior, L.; Ibrahim, S.A.; Vieira, R.P. Essential Oils as Additives in Active Starch-Based Food Packaging Films: A Review. *Int J Biol Macromol* **2021**, *182*, 1803–1819, doi:10.1016/J.IJBIOMAC.2021.05.170.
10. Azman, N.H.; Khairul, W.M.; Sarbon, N.M. A Comprehensive Review on Biocompatible Film Sensor Containing Natural Extract: Active/Intelligent Food Packaging. *Food Control* **2022**, *141*, 109189, doi:10.1016/J.FOODCONT.2022.109189.
11. Burt, S. Essential Oils: Their Antibacterial Properties and Potential Applications in Foods—a Review. *Int J Food Microbiol* **2004**, *94*, 223–253, doi:10.1016/J.IJFOODMICRO.2004.03.022.
12. Nunes, J.C.; Melo, P.T.S.; Lorevice, M.V.; Aouada, F.A.; de Moura, M.R. Effect of Green Tea Extract on Gelatin-Based Films Incorporated with Lemon Essential Oil. *J Food Sci Technol* 2021, *58*.
13. Mondéjar-López, M.; Rubio-Moraga, A.; López-Jimenez, A.J.; García Martínez, J.C.; Ahrazem, O.; Gómez-Gómez, L.; Niza, E. Chitosan Nanoparticles Loaded with Garlic Essential Oil: A New Alternative to Tebuconazole as Seed Dressing Agent. *Carbohydr Polym* **2022**, *277*, 118815, doi:10.1016/j.carbpol.2021.118815.
14. Ajami, M.; Vazirijavid, R. Garlic (Allium Sativum L.). *Nonvitamin and Nonmineral Nutritional Supplements* **2019**, 227–234, doi:10.1016/B978-0-12-812491-8.00033-3.
15. de Moura, M.R.; Aouada, F.A.; Mattoso, L.H.C. Preparation of Chitosan Nanoparticles Using Methacrylic Acid. *J Colloid Interface Sci* **2008**, *321*, 477–483, doi:10.1016/J.JCIS.2008.02.006.
16. Standard test methods for tensile properties of thin plastic sheeting ASTM D882-2012. *Annual Book of American Standard Testing Methods* 2012, 313–321.

17. Mchugh, T.H.; Avena-Bustillos, F.L.; Krochta, J.M. Hydrophilic Edible Films: Modified Procedure for Water Vapor Permeability and Explanation of Thickness Effects;
18. Otoni, C.G.; Avena-Bustillos, R.J.; Azeredo, H.M.C.; Lorevice, M. v.; Moura, M.R.; Mattoso, L.H.C.; McHugh, T.H. Recent Advances on Edible Films Based on Fruits and Vegetables—A Review. *Compr Rev Food Sci Food Saf* **2017**, *16*, 1151–1169, doi:10.1111/1541-4337.12281.
19. Aranda-Barradas, M.E.; Trejo-López, S.E.; Real, A. del; Álvarez-Almazán, S.; Méndez-Albores, A.; García-Tovar, C.G.; González-Díaz, F.R.; Miranda-Castro, S.P. Effect of Molecular Weight of Chitosan on the Physicochemical, Morphological, and Biological Properties of Polyplex Nanoparticles Intended for Gene Delivery. *Carbohydrate Polymer Technologies and Applications* **2022**, *4*, 100228, doi:10.1016/J.CARPTA.2022.100228.
20. Lorevice, M. v.; de Moura, M.R.; Mattoso, L.H.C. Nanocompósito de Polpa de Mamão e Nanopartículas de Quitosana Para Aplicação Em Embalagens. *Quim Nova* **2014**, *37*, 931–936, doi:10.5935/0100-4042.20140174.
21. Ortega-Toro, R.; Jiménez, A.; Talens, P.; Chiralt, A. Effect of the Incorporation of Surfactants on the Physical Properties of Corn Starch Films. *Food Hydrocoll* **2014**, *38*, 66–75, doi:10.1016/J.FOODHYD.2013.11.011.
22. Rodríguez, M.; Osés, J.; Ziani, K.; Maté, J.I. Combined Effect of Plasticizers and Surfactants on the Physical Properties of Starch Based Edible Films. *Food Research International* **2006**, *39*, 840–846, doi:10.1016/J.FOODRES.2006.04.002.
23. Muscat, D.; Tobin, M.J.; Guo, Q.; Adhikari, B. Understanding the Distribution of Natural Wax in Starch–Wax Films Using Synchrotron-Based FTIR (S-FTIR). *Carbohydr Polym* **2014**, *102*, 125–135, doi:10.1016/J.CARBPOL.2013.11.004.
24. Basiak, E.; Debeaufort, F.; Lenart, A. Effect of Oil Lamination between Plasticized Starch Layers on Film Properties. *Food Chem* **2016**, *195*, 56–63, doi:10.1016/J.FOODCHEM.2015.04.098.
25. Zhong, Y.; Li, Y. Effects of Surfactants on the Functional and Structural Properties of Kudzu (Pueraria Lobata) Starch/Ascorbic Acid Films. *Carbohydr Polym* **2011**, *85*, 622–628, doi:10.1016/J.CARBPOL.2011.03.031.
26. Rubilar, J.F.; Zúñiga, R.N.; Osorio, F.; Pedreschi, F. Physical Properties of Emulsion-Based Hydroxypropyl Methylcellulose/Whey Protein Isolate (HPMC/WPI) Edible Films. *Carbohydr Polym* **2015**, *123*, 27–38, doi:10.1016/J.CARBPOL.2015.01.010.
27. Handayasari, F.; Suyatma, N.E.; Nurjanah, S. Physiochemical and Antibacterial Analysis of Gelatin–Chitosan Edible Film with the Addition of Nitrite and Garlic Essential Oil by Response Surface Methodology. *J Food Process Preserv* **2019**, *43*, doi:10.1111/jfpp.14265.
28. Wang, H.; Ding, F.; Ma, L.; Zhang, Y. Edible Films from Chitosan-Gelatin: Physical Properties and Food Packaging Application. *Food Biosci* **2021**, *40*, 100871, doi:10.1016/J.FBIO.2020.100871.
29. Kurek, M.; Benbettaieb, N.; Ščetar, M.; Chaudy, E.; Elez-Garofulić, I.; Repajić, M.; Klepac, D.; Valić, S.; Debeaufort, F.; Galić, K. Novel Functional Chitosan and Pectin Bio-Based Packaging Films with Encapsulated Opuntia-Ficus Indica Waste. *Food Biosci* **2021**, *41*, 100980, doi:10.1016/J.FBIO.2021.100980.
30. Jamróz, E.; Tkaczewska, J.; Juszczak, L.; Zimowska, M.; Kawecka, A.; Krzyściak, P.; Skóra, M. The Influence of Lingonberry Extract on the Properties of Novel, Double-Layered Biopolymer Films Based on Furcellaran, CMC and a Gelatin Hydrolysate. *Food Hydrocoll* **2022**, *124*, 107334, doi:10.1016/J.FOODHYD.2021.107334.
31. Oyeoka, H.C.; Ewulonu, C.M.; Nwuzor, I.C.; Obele, C.M.; Nwabanne, J.T. Packaging and Degradability Properties of Polyvinyl Alcohol/Gelatin Nanocomposite Films Filled Water Hyacinth Cellulose Nanocrystals. *Journal of Bioresources and Bioproducts* **2021**, *6*, 168–185, doi:10.1016/J.JOBAB.2021.02.009.
32. Oyekanmi, A.A.; Abdul Khalil, H.P.S.; Rahman, A.A.; Mistar, E.M.; Olaiya, N.G.; Alfatah, T.; Yahya, E.B.; Mariana, M.; Hazwan, C.M.; Abdullah, C.K. Extracted Supercritical CO2 Cinnamon Oil Functional Properties Enhancement in Cellulose Nanofibre Reinforced Euchema Cottoni Biopolymer Films. *Journal of Materials Research and Technology* **2021**, *15*, 4293–4308, doi:10.1016/J.JMRT.2021.10.025.
33. Regina, S.; Poerio, T.; Mazzei, R.; Sabia, C.; Iseppi, R.; Giorno, L. Pectin as a Non-Toxic Crosslinker for Durable and Water-Resistant Biopolymer-Based Membranes with Improved Mechanical and Functional Properties. *Eur Polym J* **2022**, *172*, 111193, doi:10.1016/J.EURPOLYMJ.2022.111193.
34. Jahromi, M.; Niakousari, M.; Golmakani, M.T. Fabrication and Characterization of Pectin Films Incorporated with Clove Essential Oil Emulsions Stabilized by Modified Sodium Caseinate. *Food Packag Shelf Life* **2022**, *32*, 100835, doi:10.1016/J.FPSL.2022.100835.
35. do Evangelho, J.A.; da Silva Dannenberg, G.; Biduski, B.; el Halal, S.L.M.; Kringel, D.H.; Gularte, M.A.; Fiorentini, A.M.; da Rosa Zavareze, E. Antibacterial Activity, Optical, Mechanical, and Barrier Properties of Corn Starch Films Containing Orange Essential Oil. *Carbohydr Polym* **2019**, *222*, 114981, doi:10.1016/J.CARBPOL.2019.114981.
36. Vianna, T.C.; Marinho, C.O.; Marangoni Júnior, L.; Ibrahim, S.A.; Vieira, R.P. Essential Oils as Additives in Active Starch-Based Food Packaging Films: A Review. *Int J Biol Macromol* **2021**, *182*, 1803–1819, doi:10.1016/J.IJBIOMAC.2021.05.170.
37. Li, Z.; Jiang, X.; Huang, H.; Liu, A.; Liu, H.; Abid, N.; Ming, L. Chitosan/Zein Films Incorporated with Essential Oil Nanoparticles and Nanoemulsions: Similarities and Differences. *Int J Biol Macromol* **2022**, *208*, 983–994, doi:10.1016/J.IJBIOMAC.2022.03.200.
38. Luo, Q.; Hossen, M.A.; Zeng, Y.; Dai, J.; Li, S.; Qin, W.; Liu, Y. Gelatin-Based Composite Films and Their Application in Food Packaging: A Review. *J Food Eng* **2022**, *313*, 110762, doi:10.1016/J.JFOODENG.2021.110762.

39. Yeddes, W.; Djebali, K.; Aidi Wannes, W.; Horchani-Naifer, K.; Hammami, M.; Younes, I.; Saidani Tounsi, M. Gelatin-Chitosan-Pectin Films Incorporated with Rosemary Essential Oil: Optimized Formulation Using Mixture Design and Response Surface Methodology. *Int J Biol Macromol* **2020**, *154*, 92–103, doi:10.1016/J.IJBIOMAC.2020.03.092.
40. Norcino, L.B.; Mendes, J.F.; Natarelli, C.V.L.; Manrich, A.; Oliveira, J.E.; Mattoso, L.H.C. Pectin Films Loaded with Copaiba Oil Nanoemulsions for Potential Use as Bio-Based Active Packaging. *Food Hydrocoll* **2020**, *106*, 105862, doi:10.1016/J.FOODHYD.2020.105862.
41. Brandelero, R.P.H.; Yamashita, F.; Grossmann, M.V.E. The Effect of Surfactant Tween 80 on the Hydrophilicity, Water Vapor Permeation, and the Mechanical Properties of Cassava Starch and Poly(Butylene Adipate-Co-Terephthalate) (PBAT) Blend Films. *Carbohydr Polym* **2010**, *82*, 1102–1109, doi:10.1016/J.CARBPOL.2010.06.034.
42. Song, X.; Zuo, G.; Chen, F. Effect of Essential Oil and Surfactant on the Physical and Antimicrobial Properties of Corn and Wheat Starch Films. *Int J Biol Macromol* **2018**, *107*, 1302–1309, doi:10.1016/J.IJBIOMAC.2017.09.114.
43. Otoni, C.G.; Pontes, S.F.O.; Medeiros, E.A.A. Edible Films from Methylcellulose and Nanoemulsions of Clove Bud (Syzygium Aromaticum) and Oregano (Origanum Vulgare) Essential Oils as Shelf Life Extenders for Sliced Bread. **2014**.
44. Bravin, B.; Peressini, D.; Sensidoni, A. Influence of Emulsifier Type and Content on Functional Properties of Polysaccharicle Lipid-Basid Edible Films. *J Agric Food Chem* **2004**, *52*, 6448–6455, doi:10.1021/jf040065b.
45. Espitia, P.J.P.; Du, W.X.; Avena-Bustillos, R. de J.; Soares, N. de F.F.; McHugh, T.H. Edible Films from Pectin: Physical-Mechanical and Antimicrobial Properties - A Review. *Food Hydrocoll* **2014**, *35*, 287–296, doi:10.1016/J.FOODHYD.2013.06.005.
46. Cazón, P.; Velazquez, G.; Ramírez, J.A.; Vázquez, M. Polysaccharide-Based Films and Coatings for Food Packaging: A Review. *Food Hydrocoll* **2017**, *68*, 136–148, doi:10.1016/J.FOODHYD.2016.09.009.
47. Aitboulahsen, M.; el Galiou, O.; Laglaoui, A.; Bakkali, M.; Hassani Zerrouk, M. Effect of Plasticizer Type and Essential Oils on Mechanical, Physicochemical, and Antimicrobial Characteristics of Gelatin, Starch, and Pectin-Based Films. *J Food Process Preserv* **2020**, *44*, doi:10.1111/jfpp.14480.
48. Myllärinen, P.; Partanen, R.; Seppälä, J.; Forssell, P. Effect of Glycerol on Behaviour of Amylose and Amylopectin Films. *Carbohydr Polym* **2002**, *50*, 355–361, doi:10.1016/S0144-8617(02)00042-5.
49. Park, H.J.; Chinnan, M.S. Gas and Water Vapor Barrier Properties of Edible Films from Protein and Cellulosic Materials. *J Food Eng* **1995**, *25*, 497–507, doi:10.1016/0260-8774(94)00029-9.
50. Chen, H. Functional Properties and Applications of Edible Films Made of Milk Proteins. *J Dairy Sci* **1995**, *78*, 2563–2583, doi:10.3168/JDS.S0022-0302(95)76885-0.
51. Martelli, M.R.; Barros, T.T.; de Moura, M.R.; Mattoso, L.H.C.; Assis, O.B.G. Effect of Chitosan Nanoparticles and Pectin Content on Mechanical Properties and Water Vapor Permeability of Banana Puree Films. *J Food Sci* **2013**, *78*, doi:10.1111/j.1750-3841.2012.03006.x.
52. Monfregola, L.; Leone, M.; Vittoria, V.; Amodeo, P.; de Luca, S. Chemical Modification of Pectin: Environmental Friendly Process for New Potential Material Development. *Polym Chem* **2011**, *2*, 800–804, doi:10.1039/c0py00341g.
53. Cerruti, P.; Santagata, G.; Gomez D'Ayala, G.; Ambrogi, V.; Carfagna, C.; Malinconico, M.; Persico, P. Effect of a Natural Polyphenolic Extract on the Properties of a Biodegradable Starch-Based Polymer. *Polym Degrad Stab* **2011**, *96*, 839–846, doi:10.1016/J.POLYMDEGRADSTAB.2011.02.003.
54. Rejinold, N.S.; Muthunarayanan, M.; Muthuchelian, K.; Chennazhi, K.P.; Nair, S. v.; Jayakumar, R. Saponin-Loaded Chitosan Nanoparticles and Their Cytotoxicity to Cancer Cell Lines in Vitro. *Carbohydr Polym* **2011**, *84*, 407–416, doi:10.1016/J.CARBPOL.2010.11.056.
55. Thandapani, G.; Supriya Prasad, P.; Sudha, P.N.; Sukumaran, A. Size Optimization and in Vitro Biocompatibility Studies of Chitosan Nanoparticles. *Int J Biol Macromol* **2017**, *104*, 1794–1806, doi:10.1016/J.IJBIOMAC.2017.08.057.
56. Feng, Y.; Xia, W. Preparation, Characterization and Antibacterial Activity of Water-Soluble O-Fumaryl-Chitosan. *Carbohydr Polym* **2011**, *83*, 1169–1173, doi:10.1016/J.CARBPOL.2010.09.026.
57. Moghimi, R.; Ghaderi, L.; Rafati, H.; Aliahmadi, A.; Mcclements, D.J. Superior Antibacterial Activity of Nanoemulsion of Thymus Daenensis Essential Oil against E. Coli. *Food Chem* **2016**, *194*, 410–415, doi:10.1016/J.FOODCHEM.2015.07.139.
58. Medina Jaramillo, C.; Gutiérrez, T.J.; Goyanes, S.; Bernal, C.; Famá, L. Biodegradability and Plasticizing Effect of Yerba Mate Extract on Cassava Starch Edible Films. *Carbohydr Polym* **2016**, *151*, 150–159, doi:10.1016/J.CARBPOL.2016.05.025.
59. Ross, Z.M.; O'Gara, E.A.; Hill, D.J.; Sleightholme, H. v.; Maslin, D.J. Antimicrobial Properties of Garlic Oil against Human Enteric Bacteria: Evaluation of Methodologies and Comparisons with Garlic Oil Sulfides and Garlic Powder. *Appl Environ Microbiol* **2001**, *67*, 475–480, doi:10.1128/AEM.67.1.475-480.2001.
60. Yuan, G.; Chen, X.; Li, D. Chitosan Films and Coatings Containing Essential Oils: The Antioxidant and Antimicrobial Activity, and Application in Food Systems. *Food Research International* **2016**, *89*, 117–128, doi:10.1016/J.FOODRES.2016.10.004.
61. Pranoto, Y.; Salokhe, V.M.; Rakshit, S.K. Physical and Antibacterial Properties of Alginate-Based Edible Film Incorporated with Garlic Oil. In Proceedings of the Food Research International; April 2005; Vol. 38, pp. 267–272.